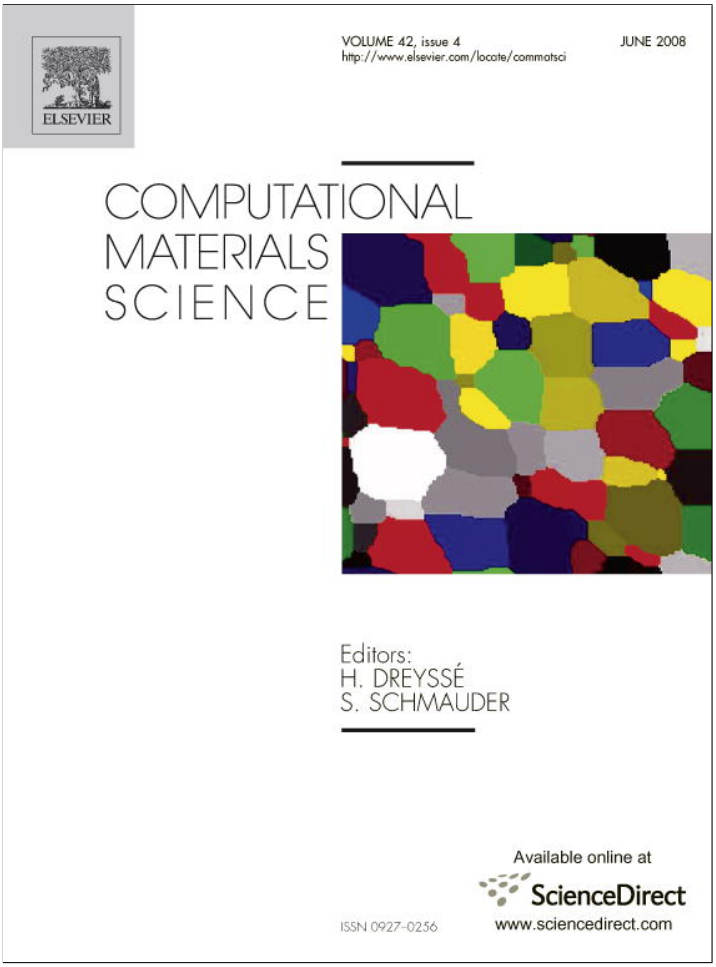

Available online at www.sciencedirect.com
ScienceDirect
Computational Materials Science 42 (2008) 704–712
COMPUTATIONAL MATERIALS SCIENCE
www.elsevier.com/locate/commatsci

Computational homogenization for nonlinear conduction in heterogeneous materials using model reduction

E. Monteiro, J. Yvonnet *, Q.C. He

Université Paris-Est, Laboratoire de Mécanique (LAM-EA2545), 5 bd Descartes, 77454 Marne-la-Vallée Cedex 2, France

Received 30 January 2007; received in revised form 27 September 2007; accepted 5 November 2007
Available online 21 February 2008

Abstract

In the present work, we propose a method combining a multi-scale approach and a model reduction technique based on proper orthogonal decomposition (POD) to solve highly nonlinear conduction problems in structures made of periodic heterogeneous materials. Following classical computational homogenization schemes, a representative volume element is associated with each integration point of the macrostructure. The local macroscopic response is computed directly on the RVE through solving an incremental problem with appropriate boundary and initial conditions. In the proposed method, the equations of the linearized micro problem are projected on the reduced basis, which is obtained using POD via preliminary computations. The set of unknowns and Lagrange multipliers associated with periodic boundary conditions is largely reduced. The technique called reduced model multi-scale method (R3M) lowers the computational costs. Both accuracy and efficiency are examined through numerical tests involving thermal and electric nonlinear conduction problems.

PACS: 02.30.Jr; 02.70.Dh; 02.70.−c; 46.15.−x; 47.11.St; 51.20.+d

Keywords: Computational homogenization; Multi-scale method; Nonlinear conduction; POD; Model reduction

1. Introduction

Predicting the effective properties of heterogeneous materials, such as composites with nonlinear behaviour, is crucial in many applications. Homogenization techniques have been successfully developed for linear materials but they still remain limited in nonlinear cases.

Available homogenization approaches provide rigorous bounds for the effective properties of nonlinear heterogeneous materials through an appropriate extension of variational principles [1–4]. However, analytical theories are restricted in many circumstances due to complex geometries or complex constitutive laws.

In order to overcome this difficulty, computational homogenization methods have been worked out recently [5–12]. When scale separation prevails, direct simulations on the whole structure by meshing all heterogeneities may be not practicable even using parallel computing, whereas multi-scale homogenization algorithm can be applied to obtain effective material properties. This kind of technique [7–12] requires the resolution of two boundary value problems at the same time: one at the macro scale and another at the micro level. This approach, however, remains computationally expensive, as a nonlinear problem has to be solved at each macroscopic integration point.

Alternatively, computational cost can be reduced by mean of a model reduction based on proper orthogonal decomposition (POD) (see e.g. [13–16]). The POD is a powerful method to capture correlation between sequences of data sets, extracting only pertinent information with a few number of modes.

The central goal of this study is to adapt a reduced model multi-scale method [12] to transient conduction in nonlinear heterogeneous media. In this context, the macroscopic gradient is first computed at every macroscopic

* Corresponding author.
E-mail address: j.yvonnet@univ-mlv.fr (J. Yvonnet).

0927-0256/$ - see front matter © 2007 Elsevier B.V. All rights reserved.
doi:10.1016/j.commatsci.2007.11.001

point and then used to formulate appropriate boundary conditions for a representative volume element (RVE). The resolution of the nonlinear microscopic problem, employing a reduced model obtained by preliminary computations, provides a local macroscopic response through averaged fields.

In the present paper, the multi-scale transient conduction problem is formulated in Section 2. Details on model reduction based on POD are given in Section 3. Finally, numerical examples involving nonlinear thermal and electrical conduction problems are presented in Section 4 to examine accuracy and efficiency of the method.

2. Formulation of the multi-scale transient conduction problem

We consider a heterogeneous material with periodic microstructure depicted in Fig. 1. We define two distinct scales. One is the scale of the heterogeneities. The other is the macro scale where the material can be assumed homogeneous. In this section, we formulate the problem at each scale.

2.1. Macro problem

Let Ω be an open domain occupied by the equivalent homogeneous body bounded by $\partial\Omega$ which is decomposed into two disjoint complementary parts $\partial\Omega_u$ and $\partial\Omega_q$ where essential and natural boundary conditions are prescribed respectively. Let $\bar{u}(\bar{\mathbf{x}},t)$ be a scalar field, depending on the macroscopic coordinates $\bar{\mathbf{x}} \in \Omega \cup \partial\Omega$ and on the time $t \in [0;\infty[$, solution of the nonlinear transient conduction problem governed by

$$\bar{c}(\bar{u})\dot{\bar{u}}(\bar{\mathbf{x}},t) + \operatorname{div}\bar{\mathbf{q}}(\bar{u}) - \bar{g} = 0, \quad \bar{\mathbf{x}} \in \Omega, \tag{1}$$

$$\bar{u}(\bar{\mathbf{x}},t) = \tilde{u}, \quad \bar{\mathbf{x}} \in \partial\Omega_u, \tag{2}$$

$$\bar{\mathbf{q}}(\bar{u}) \cdot \mathbf{n} = \tilde{q}, \quad \bar{\mathbf{x}} \in \partial\Omega_q, \tag{3}$$

$$\bar{u}(\bar{\mathbf{x}},t=0) = u^0, \quad \bar{\mathbf{x}} \in \Omega, \tag{4}$$

where $\bar{c}$, $\bar{g}$ and $\mathbf{n}$ denote a material property, a volumetric source and the unit outward normal vector on $\partial\Omega$, respectively. The flux related to $\bar{u}$ is noted $\bar{\mathbf{q}}$. Boundary and initial conditions are prescribed through $\tilde{u}$, $\tilde{q}$ and u^0. The superposed dot is used to denote time differentiation. In the following, the brackets indicating that $\bar{u}$ depends on space and time are omitted, for the sake of conciseness.

The variational formulation associated with the balance energy Eq. (1), is given by

Find $\bar{u} \in \mathscr{S}(\Omega)$ satisfying conditions (2) and (4), such that $\forall \delta\bar{v} \in \mathscr{S}_0(\Omega)$,

$$\int_\Omega \bar{c}(\bar{u})\dot{\bar{u}}\delta\bar{v}\,\mathrm{d}\Omega - \int_\Omega \bar{\mathbf{q}}(\bar{u}) \cdot \mathit{grad}\,\delta\bar{v}\,\mathrm{d}\Omega = \int_\Omega \bar{g}\delta\bar{v}\,\mathrm{d}\Omega - \int_{\partial\Omega_q} \tilde{q}\delta\bar{v}\,\mathrm{d}S \tag{5}$$

or in a more compact form

$$\mathscr{R}(\bar{u},\delta\bar{v}) = 0, \tag{6}$$

where $\mathscr{S}(\Omega)$ and $\mathscr{S}_0(\Omega)$ are appropriate Sobolev spaces [17,18].

Using a standard finite element discretization in tandem with an implicit time integration scheme, the relation (6) leads to a set of nonlinear equations which requires an incremental procedure, e.g. Newton–Raphson, to be solved. The macroscopic mesh associated with this problem is plotted in Fig. 2. However, it should be emphasized that the relation between $\bar{q}$ and $\bar{u}$ is unknown at this scale. To determine this relation, we introduce the microscopic problem.

2.2. Micro problem

Let Ω^μ be an open domain with boundary $\partial\Omega^\mu$ describing a representative volume element associated with the neighbourhood of a macroscopic point $\bar{\mathbf{x}}$. The equations governing the nonlinear transient conduction in Ω^μ are identical to (1)–(6), where provided micro quantities replace macro ones without $\bar{(\cdot)}$. At this scale, we assume that materials properties of each phase are known. In this work, we consider a nonlinear thermal conduction problem in which a nonlinear generalized Fourier law

$$\mathbf{q}(u) = -\mathbf{K}(u) \cdot \mathit{grad}\,u \tag{7}$$

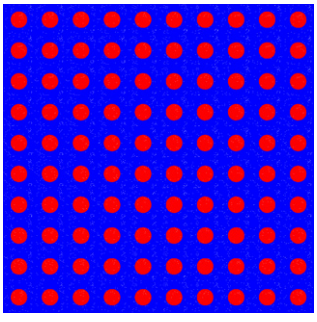

Fig. 1. Full structure.

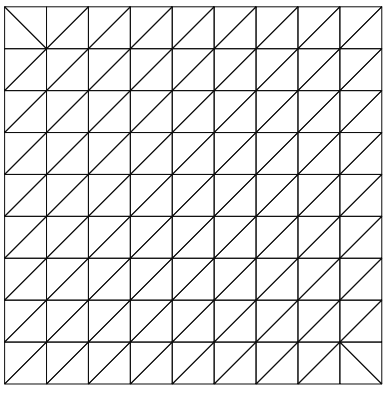

Fig. 2. Macroscopic mesh.

is adopted, and a nonlinear electrical conduction problem in which a power law

$$\mathbf{q}(u) = -\boldsymbol{\chi}\|grad\, u\|^{p-1} grad\, u \tag{8}$$

is more adapted (see e.g. Refs. [1,2,4]). In those relations, $\mathbf{K}(u)$ represents a second order tensor whose components depend on u while $\boldsymbol{\chi}$ and p denote the second order anisotropic nonlinear susceptibility tensor and the nonlinearity index, respectively.

To solve the nonlinear problem at the micro scale by the Newton–Raphson algorithm, it is necessary to establish the linearized conduction problem which reads

$$D_{\Delta u}\mathscr{R}(u,\delta v) = -\mathscr{R}(u,\delta v) \tag{9}$$

where $D_{\Delta u}(.)$ denotes the directional derivative (Gâteau operator) of $\mathscr{R}(u,\delta v)$ at any fixed u in the direction of Δu. For a more detailed account on directional derivative, the reader is referred to [19]. After finite element discretization of (9), we obtain the following system:

$$[K_T]\{\Delta u\} = -\{R\}, \tag{10}$$

where $[K_T]$ and $\{R\}$ denote the tangent matrix and the residual vector, respectively.

To complete the micro problem, we need to specify boundary and initial conditions. Those points are detailed below.

2.3. Link between the two scales

One main ingredient of computational homogenization is to consider a RVE for each integration point of the macroscopic mesh. The coupling between the micro and macro scales is ensured by boundary and initial conditions imposed on the RVE and by the estimation of macroscopic unknown quantities such as $\bar{\mathbf{q}}$, $\bar{c}$ and the macroscopic tangent matrix through averaging the different microscopic quantities.

For this purpose, we assume that the microscopic solution u is the superposition of an average field from the macro domain and a fluctuation w induced by the heterogeneities

$$u(\mathbf{x},t) = \overline{grad\, u(t)} \cdot \mathbf{x} + w(\mathbf{x},t), \tag{11}$$

where $\mathbf{x}$ denotes a generic point in the micro domain. Applying the gradient operator and taking the volume average over Ω^μ, we obtain

$$\frac{1}{|\Omega^\mu|}\int_{\Omega^\mu} grad\, u\, d\Omega = \frac{1}{|\Omega^\mu|}\int_{\Omega^\mu} \overline{grad\, u}\, d\Omega + \frac{1}{|\Omega^\mu|}\int_{\Omega^\mu} grad\, w(\mathbf{x}) d\Omega, \tag{12}$$

which requires

$$\frac{1}{|\Omega^\mu|}\int_{\Omega^\mu} grad\, w(\mathbf{x}) d\Omega = \frac{1}{|\Omega^\mu|}\int_{\partial\Omega^\mu} w(\mathbf{x})\ \mathbf{n}^\mu\, dS = 0, \tag{13}$$

where $\mathbf{n}^\mu$ denotes the unit outward normal on $\partial\Omega^\mu$. Condition (13) is satisfied for the following boundary conditions:

$$w(\mathbf{x}) = 0 \text{ on } \partial\Omega^\mu \quad \text{or} \quad w(\mathbf{x}^+) = w(\mathbf{x}^-) \text{ on } \partial\Omega^\mu, \tag{14}$$

where $\mathbf{x}^+$ and $\mathbf{x}^-$ denote two opposite points on a rectangular boundary $\partial\Omega^\mu$. The first equation in (14) is verified by using homogeneous essential boundary conditions

$$u = \overline{grad\, u} \cdot \mathbf{x} \text{ on } \partial\Omega^\mu, \tag{15}$$

whereas, the second equation corresponds to periodic boundary conditions for the fluctuation implying the decomposition of $\partial\Omega^\mu$ into two disjoint complementary parts $\partial\Omega^{\mu+}$ and $\partial\Omega^{\mu-}$ associated with $\mathbf{x}^+$ and $\mathbf{x}^-$, respectively. In this study, we focus on the periodic boundary conditions which may be stated as follows:

$$u^+ - u^- = \overline{grad\, u} \cdot (\mathbf{x}^+ - \mathbf{x}^-) \text{ on } \partial\Omega^\mu, \tag{16}$$

where u^+ and u^- denote the solution of the microscopic conduction problem at points $\mathbf{x}^+$ and $\mathbf{x}^-$, respectively.

After solving the microscopic problem, the macroscopic flux is computed by

$$\bar{\mathbf{q}} = \frac{1}{|\Omega^\mu|}\int_{\Omega^\mu} \mathbf{q}\, d\Omega \tag{17}$$

while, according to [6], the macroscopic dynamic property is recovered through

$$\bar{c} = \frac{1}{|\Omega^\mu|}\int_{\Omega^\mu} c^{(r)}\, d\Omega, \tag{18}$$

where the superscript r denotes the corresponding constituent phase ($r = 1$ for the matrix material and $r = 2$ for the inclusions). It should be underlined that, in this approach, no assumption on the form of $\bar{\mathbf{q}}$ and $\bar{c}$ is needed, which allows to take very different and complicated microscopic constitutive laws and arbitrary periodic microgeometry.

Our last goal in this section is to estimate the macroscopic tangent matrix. For this purpose, we use a perturbation method as described in [7]. We calculate the microscopic response to a small variation of each component of boundary conditions. This way of calculating requires the solution of three (2D) or four (3D) finite element problems for the micro mesh whose cost is not negligible. In the following, we aim at reducing the costs associated with the plentiful nonlinear problems at the micro scale. For this purpose, we introduce model reduction for solving the microscopic problems.

3. Model reduction

The model reduction based on POD is an elegant method to alleviate computational costs. The POD process, also known as principal component analysis (PCA) or Karhunen–Loève (KL) expansion [13,15,16], is a technique which captures the overall behaviour of a physical system. The POD identifies an optimal set of orthogonal basis functions to achieve a satisfactory approximation of systems in the least square sense. The mathematical theory relies on properties of Hilbert spaces.

3.1. POD

Let $\{u(t)\} \in \mathbb{R}^N$ be a time-dependent vector field over Ω^μ, given by solving the discretized transient conduction problem at the micro level. It can be expressed as

$$\{u(t)\} = [\Phi]\{\xi(t)\}, \tag{19}$$

where $[\Phi] = [\{\phi_1\}, \{\phi_2\}, \ldots, \{\phi_N\}]$ is an arbitrary orthonormal basis of $\mathbb{R}^N$ and $\{\xi(t)\}$ are coefficients.

In the POD context, we aim at replacing $\{u(t)\}$ by an approximate solution $\{\hat{u}(t)\} = [\widehat{\Phi}]\{\hat{\xi}(t)\}$, using only M basis vectors ($M \ll N$), which satisfies

$$\underset{\{\phi_i\}}{\text{Min}} \|\{u(t)\} - \{\hat{u}(t)\}\|^2 \tag{20}$$

with the constraints

$$\langle \{\phi_i\}, \{\phi_j\} \rangle = \delta_{ij}, \tag{21}$$

where $\{\phi_i\}$ denotes the ith vector of $[\Phi]$.

It can be shown that the problem described by (20) and (21) leads to the following eigenvalue problem:

$$[V]\{\phi_i\} = \mu_i\{\phi_i\} \quad i = 1, 2, \ldots, N, \tag{22}$$

where $[V]$ is the correlation matrix defined by

$$[V] = [Q][Q]^{\mathrm{T}}, \tag{23}$$

where $[Q]$ is a $N \times S$ matrix such that

$$[Q] = [\{u(1)\}\{u(2)\}\cdots\{u(S)\}], \tag{24}$$

$\{u(t)\}$ being solutions known for S time-steps from preliminary computations. For a more detailed account, the reader is referred to [15].

Then, the reduced basis $[\widehat{\Phi}]$ is obtained by keeping only M eigenvectors of $[\Phi]$ associated with the first M higher eigenvalues μ_i. As the error induced by the approximation $\{\hat{u}(t)\}$ is estimated by

$$\|\{u(t)\} - \{\hat{u}(t)\}\| = \left(\sum_{i=M+1}^{N} \mu_i \right)^{\frac{1}{2}}, \tag{25}$$

the number M of selected basis functions, called modes in the following, is thus chosen according to the error criterion:

$$\frac{\left(\sum_{i=M+1}^{N} \mu_i\right)^{\frac{1}{2}}}{\left(\sum_{i=1}^{N} \mu_i\right)^{\frac{1}{2}}} < \delta, \tag{26}$$

where δ denotes a tolerance error parameter smaller than one. In practise, the eigenvalues quickly decrease, and only a small number of eigenvectors needs to be retained.

3.2. POD and Lagrange multipliers

Discretization of the nonlinear transient conduction problem results in an incremental discrete system of N linear equations whose matrix form is given by (10). In this context, the periodicity condition (16) can be rewritten in an incremental form

$$\Delta u^+ - \Delta u^- = 0. \tag{27}$$

Here, condition (27) is imposed by using Lagrange multipliers. The new system to be solved is in the form

$$\begin{bmatrix} [K_{\mathrm{T}}] & [G^{\mathrm{T}}] \\ [G] & [0] \end{bmatrix} \begin{Bmatrix} \{\Delta u\} \\ \{\Delta\lambda\} \end{Bmatrix} = -\begin{Bmatrix} \{R\} \\ \{0\} \end{Bmatrix}, \tag{28}$$

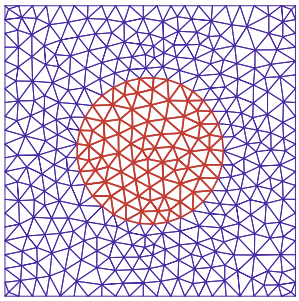

Fig. 3. Representative volume element.

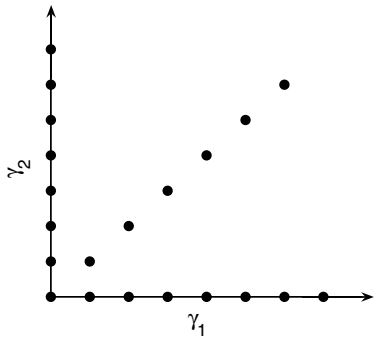

Fig. 4. Sampling points in the parameter space used to construct the POD solution.

Table 1
Coefficients of electric properties

	a_0	a_1	a_2	a_3	a_4
Matrix	500	2×10^{-1}	3×10^{-3}	1×10^{-6}	1×10^{-10}
Inclusion	100	-5×10^{-2}	-4×10^{-4}	5×10^{-7}	2×10^{-7}

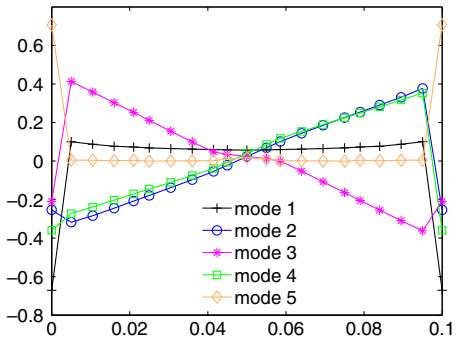

Fig. 5. Profiles of the first five modes along a line tangent to the inclusion.

where additional unknowns, the Lagrange multipliers $\{\Delta\lambda\}$, must be also reduced in the form of (19) in the framework of POD analysis.

We have noted that the Newton–Raphson algorithm used to solve the reduced linearized problem diverges when solutions $\{\tilde{u}\}$, including Lagrange multipliers, of the full microscopic problem are used to construct the reduced basis in the procedure described in Section 3.1 To overcome this issue, we propose here to project the linearized equations on a reduced basis that is built using the unknown increments $\{\Delta\tilde{u}\}$, including Lagrange multipliers, instead of the unknown $\{\tilde{u}\}$, such as we define the new matrix $[Q]$ by

$$[Q] = \begin{bmatrix} \{\Delta u_1^1\} & \cdots & \{\Delta u_1^{k^1}\} & \cdots & \{\Delta u_S^{k^S}\} \\ \{\Delta \lambda_1^1\} & \cdots & \{\Delta \lambda_1^{k^1}\} & \cdots & \{\Delta \lambda_S^{k^S}\} \end{bmatrix}, \tag{29}$$

where the superscript, the subscript and k denote iteration index, time-step and the last iteration at each time-step, respectively. Thus, in the POD context, the unknown increments $\{\Delta\tilde{u}\}$ take the following form:

$$\{\Delta\tilde{u}\} = [\widehat{\Phi}]\{\Delta\hat{\xi}\}. \tag{30}$$

Introducing (30) in (9) and expanding δv using (30), we obtain

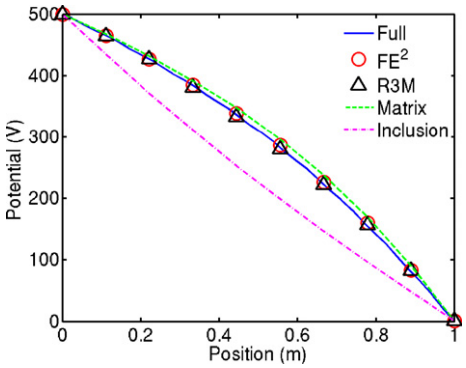

Fig. 6. Electric potential along a centered line.

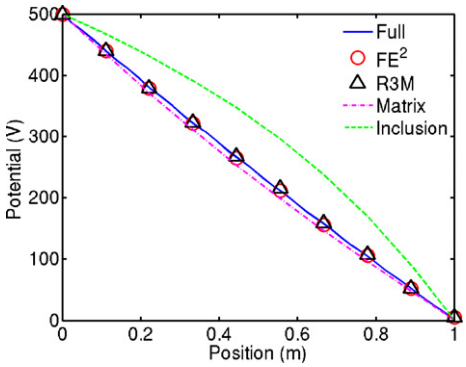

Fig. 7. Electric potential after interchanging materials properties.

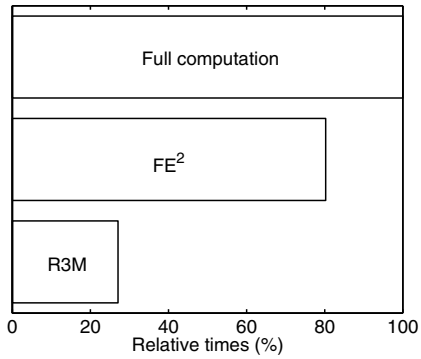

Fig. 8. Computation times.

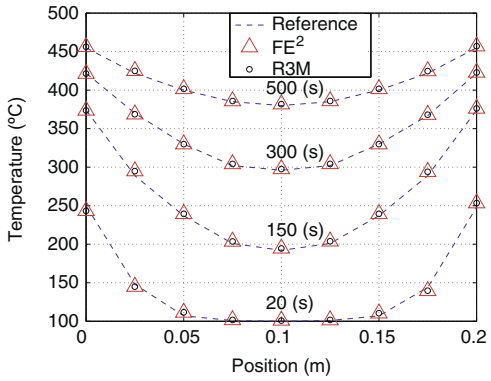

Fig. 9. Temperature distribution.

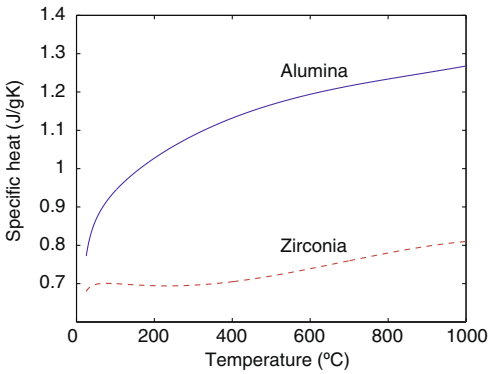

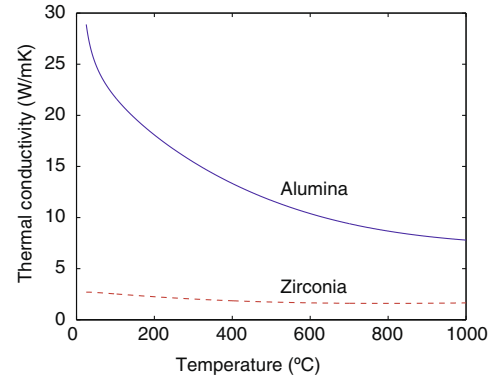

Fig. 10. Materials properties.

$$[\widehat{\Phi}]^{\mathrm{T}}[K_{\mathrm{T}}]\,[\widehat{\Phi}]\{\Delta\hat{\xi}\} = -[\widehat{\Phi}]^{\mathrm{T}}\{R\}. \tag{31}$$

This equivalent problem involves only M equations and M unknowns instead of N, with $M \ll N$. The expected computational gains are due to (a) the storage and decomposition of only small matrices and vectors associated with the linearized problem at micro scale, (b) the assembly of reduced elementary matrices instead of premultiplying the full assembled matrix by the reduced basis (see Ref. [14]).

3.3. Construction of the reduced basis

Up to now, we have not precised how to construct the reduced basis. Let $\boldsymbol{\zeta} = \{\gamma_1, \gamma_2, \ldots, \gamma_r\}$, $\boldsymbol{\zeta} \in \mathbb{R}^r$ the space of the parameters defining the system solution. In the proposed approach, we first define a set of S points in $\boldsymbol{\zeta}$, in which we solve the full problem. We then collect all the increments in the matrix $[Q]$, solve the eigenvalue problem (22) and select the M relevant eigenvectors of $[V]$ according to the criterion (26), to form the reduced basis $[\widehat{\Phi}]$. We then assume that the basis is rich enough to capture accurately the different feature of the full problem solution for any set of parameters in $\boldsymbol{\zeta}$. The steps of the reduced basis construction are summarized as follows:

(i) define S points in the r-dimensional space of the parameters $\boldsymbol{\zeta} = \{\gamma_1, \gamma_2, \ldots, \gamma_r\}$ describing the system;
(ii) solve the full problems associated with the S sets of parameters and store the increments in $[Q]$ (29);
(iii) solve the eigenvalue problem (22);
(iv) select the M relevant eigenvectors of $[V]$ according to the criterion (26) to form $[\widehat{\Phi}]$.

Here, the system of interest is the RVE, which solution is defined by two parameters $\{\gamma_1, \gamma_2\}$, the components of $\overline{grad\,u}$ in (16). In the parameter space, we define series of sampling points by $S_1 = \{\gamma_1, 0\}$, $S_2 = \{0, \gamma_2\}$ and $S_3 = \{\gamma_1, \gamma_2\}$. To determine the values of those parameters, a preliminary simulation on the macroscopic domain using a volume average of material properties is conducted. During this simulation, we store the maximum and the minimum of each component of the gradient so that the amplitudes of γ_i are picked between those values. An illustration of the sampling points used to define the S full problems is depicted in Fig. 4. It is worth noting that other strategies can be adopted to define the S points (regular grids, patters, random clouds, etc.).

4. Numerical examples

4.1. Nonlinear electrical steady conduction

Numerical computations are carried out for a unit square plate divided into triangular elements with linear interpolations. The macroscopic mesh described in Fig. 2 is composed of 100 nodes and 162 elements. The RVE is a single square with a centred circular inclusion shown in Fig. 3. It involves 423 degrees of freedom and 760 linear elements. Here, we restrict ourselves to solve electrical steady problems.

We impose a potential difference of 500 V between two opposite sides of the macroscopic domain ($\bar{x} = 0$) and ($\bar{x} = 1$) whereas, on the other sides, we assume that $\bar{\mathbf{q}} = 0$. We also suppose that the materials, forming the matrix and inclusions, obey isotropic constitutive laws which are a combination of (7) and (8), so that the electric flux reduces to

$$\mathbf{q}(u) = -(a_0 + a_1 u + a_2 u^2 + a_3 u^3)\,grad\,u + a_4 \|grad\,u\|^{p-1}\,grad\,u. \tag{32}$$

We choose arbitrarily the same nonlinearity index $p = 4$ for each phase. The other coefficients are provided in Table 1.

As described in Section 3.3, we perform preliminary computations to build the reduced basis following the three series established previously. By taking $\delta = 10^{-6}$ in (26), only 8 modes are retained. Hence, the microscopic reduced problem only involves 8 unknowns. The profiles of the first five modes along a line tangent to the inclusion are depicted in Fig. 5. Then, we carry out three simulations: one using a simple multi-scale procedure termed as FE^2 and one using a multi-scale algorithm in tandem with a model reduction termed as R3M. The last calculation, used as a reference solution, is carried out on the complete structure depicted in Fig. 1.

In Fig. 6, we compare the potential obtained along a centered line of the macroscopic domain. Good accuracy of the proposed method with respect to a full computation or a direct computational homogenization (FE^2) is observed. To check the validity of our solutions, we also plot, in the same figure, the solution of homogeneous problems in which the macroscopic plate would be only composed by the matrix material or the inclusion one. As expected, the presence of inclusions which are less conductive lowers the conductivity of the equivalent material.

Table 2
Coefficients of thermal properties

	α_0	α_1	α_2	α_3	α_4
k_{alumina}	23.6	-3.68×10^{-2}	2.85×10^{-5}	-7.73×10^{-9}	155
k_{zirconia}	2.91	3.90×10^{-3}	3.60×10^{-6}	-9.55×10^{-10}	−2.86
Cp_{alumina}	0.899	8.91×10^{-4}	-8.43×10^{-7}	3.24×10^{-10}	−3.71
Cp_{zirconia}	0.737	-3.22×10^{-4}	7.75×10^{-7}	-3.78×10^{-10}	−1.12

As a second example, we solve the same problem interchanging the materials properties. Thus, we determine the new reduced basis and perform the three same simulations. As previously, we compare in Fig. 7 our numeric solutions along the same centered line and we plot the solution of homogeneous problems. Good agreement is obtained compared to a full computation. This time, the presence of conductive inclusions increases the conductivity of the equivalent material. Besides, in Fig. 8, we compare computation times for the first case: a large reduction of the computational costs is noticed.

4.2. Nonlinear thermal transient conduction

4.2.1. Homogeneous problem

In the context of transient conduction problems, we first validate the R3M procedure for homogeneous materials. In this example, we solve a thermal transient conduction problem on a rectangular plate whose length and width are 0.2 m and 0.1 m, respectively. The surface is divided into 64 linear triangular elements which involves 45 nodes. The boundary conditions are as follow.

We impose free convection conditions on two opposite sides ($\bar{x} = 0$) and ($\bar{x} = 0.2$) of the macroscopic mesh with a heat transfer coefficient $h = 2000\ \mathrm{W\ m^{-2}\ K^{-1}}$. The other two opposite sides are assumed to be adiabatic. The initial temperature for the whole structure is equal to 100 °C while the ambient temperature is 500 °C.

We consider a homogeneous RVE whose mass density and specific heat are $7800\ \mathrm{kg\ m^{-3}}$ and $440\ \mathrm{J\ kg^{-1}\ K^{-1}}$, respectively. The constitutive equation takes the form of (7) where the heat conductivity tensor is defined by

$$\mathbf{K}(u) = (98.43 - 0.09155u + 0.255410^{-4}\ u^2)\mathbf{I}, \tag{33}$$

where $\mathbf{I}$ is the second order identity tensor.

We perform preliminary computations as detailed in Section 3.3 with $\delta = 10^{-6}$ in (26) in order to obtain a reduced basis. Only 6 modes are selected. Then, as previously, we carry out two simulations: one using the FE^2 method and one using the R3M. Results, depicted in Fig. 9, agree well with the reference solutions obtained in [20].

4.2.2. Heterogeneous problem

This last example deals with heat conduction inside ZrO_2–Al_2O_3 composite.

The macroscopic domain is the same as used in example 4.1. The RVE is a square domain with a centred circular inclusion whose volume fraction is 0.2. The matrix is assumed to be yttria-stabilized zirconia whose mass density is $5.9 \times 10^3\ \mathrm{kg\ m^{-3}}$ whereas the inclusions are made of alumina whose density is $3.9 \times 10^3\ \mathrm{kg\ m^{-3}}$. Thermal properties, i.e thermal conductivity and specific heat depicted in Fig. 10, are assumed to be functions of the temperature. In [21,22], experimental data allow to propose the following form:

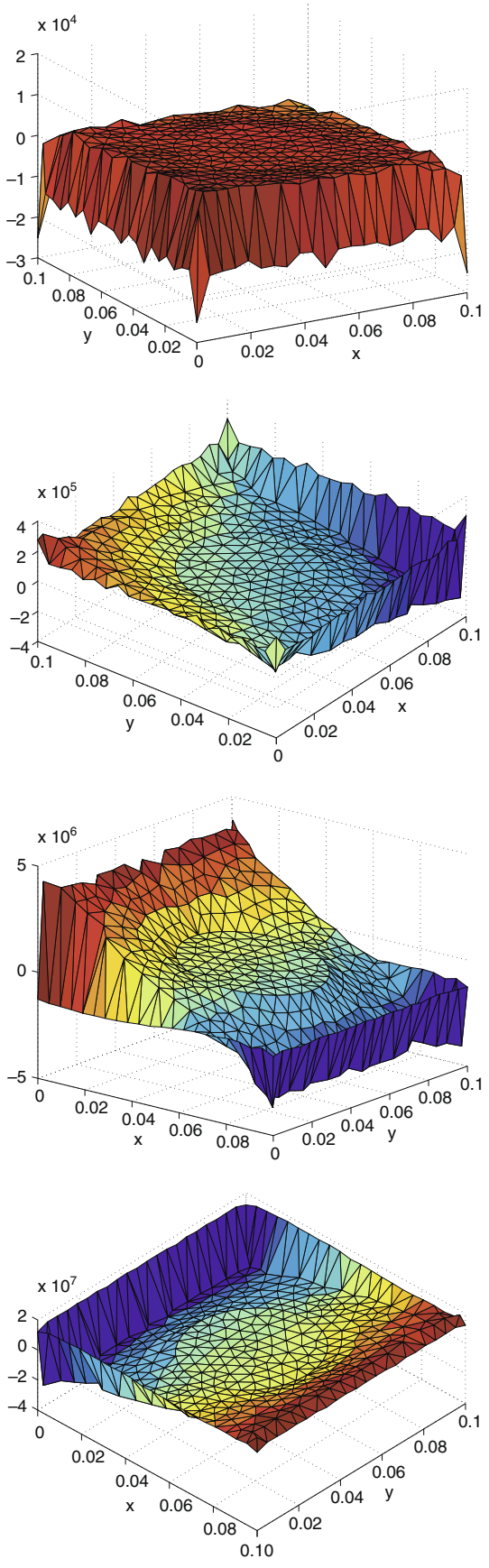

Fig. 11. Four modes selected using the POD approach.

$$\alpha_0 + \alpha_1 u + \alpha_2 u^2 + \alpha_3 u^3 + \alpha_4 u^{-1}, \tag{34}$$

which covers a large number of isotropic conductivity and specific heat forms used in thermal problems. The different coefficients are given in Table 2.

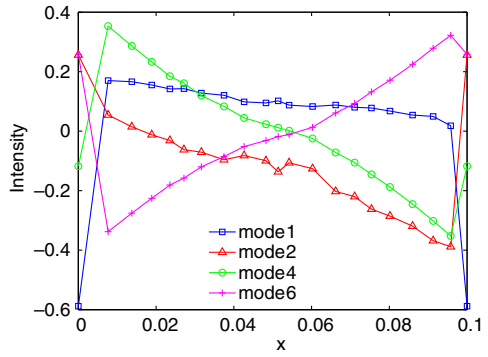

Fig. 12. Profiles of four modes along a line ($y = 0.02$).

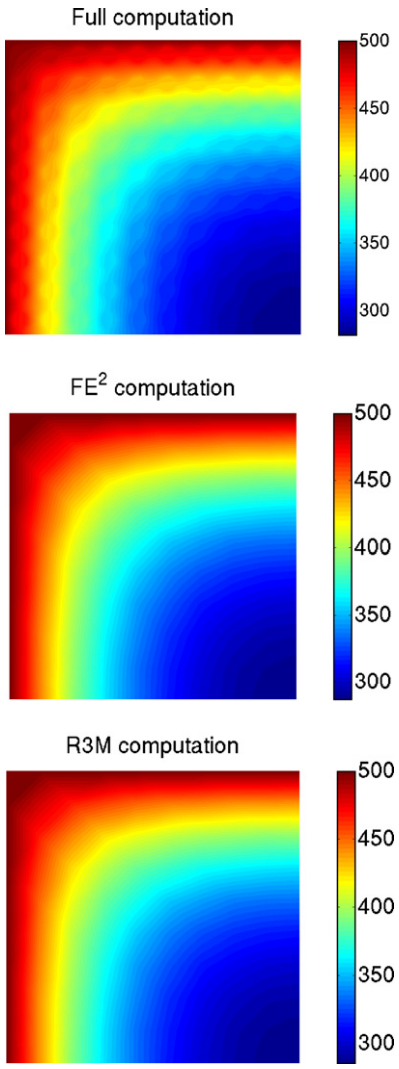

Fig. 13. Temperature distribution.

We impose on the sides ($\bar{x} = 0$) and ($\bar{y} = 1$) of the macroscopic mesh a temperature of 500 °C whereas the other sides are subjected to an adiabatic condition. The initial temperature of the structure is taken to be uniform and equal to 100 °C.

In order to obtain a reduced basis, we perform preliminary computations as detailed in Section 3.3 with $\delta = 10^{-6}$ in (26). The microscopic reduced problem involves only 7 unknowns instead of 480 (439 for the temperature unknowns and 41 for Lagrange multipliers associated with boundary conditions). Four modes are depicted in Fig. 11 while Fig. 12 shows the functional profile of those 4 modes

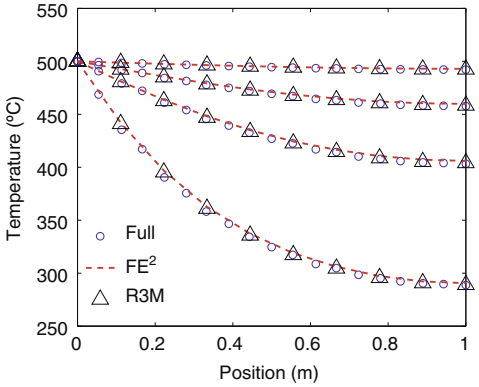

Fig. 14. Temperature distribution along $\bar{y} = 0.22$ m for different time-steps.

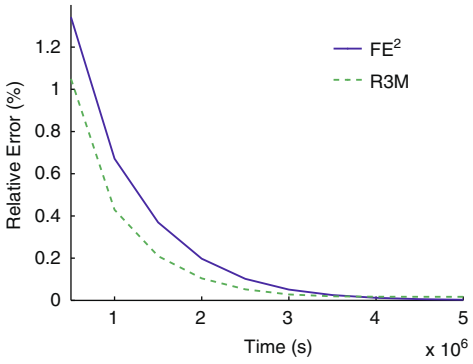

Fig. 15. Relative error.

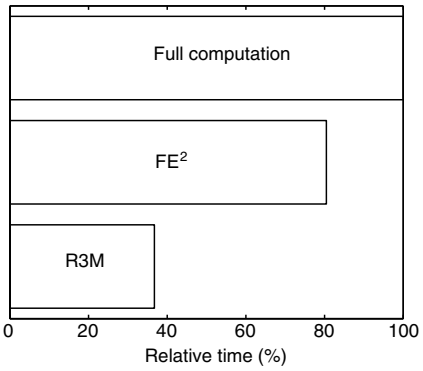

Fig. 16. Time computations.

along a line ($y = 0.02$). The Lagrange multipliers fields are not represented.

Then, we carry out three simulations: two multi-scale computations as previously described and one where the whole heterogeneous structure is meshed (see Fig. 1). The latter is used as a reference solution. The numerical results are shown in Fig. 13. Good agreement between the different methods is noticed.

In Fig. 14, we compare the homogenized temperature obtained through the different approaches along a line ($\bar{\mathbf{y}} = 0.22$) at different time-steps. The relative error in percent, given by

$$e = 100\frac{\|T - T^{\text{ref}}\|}{\|T^{\text{ref}}\|}, \tag{35}$$

where T and T^{ref} denote the temperature obtained through multi-scale and full computations respectively, is depicted in Fig. 15. A good agreement with the reference solution is observed.

We also compare computation times in Fig. 16. Once again, important reduction of computational times is achieved in comparison with a simple multi-scale method.

5. Conclusion

In this work, a reduced model multi-scale method (R3M) initially developed for solid mechanics problems in [12] has been applied to solve highly nonlinear conduction problems. The proposed method lowers computational costs with regard to brute computation or simple multi-scale computations as the total degrees of freedom (unknowns of the nonlinear microscopic problem and Lagrange multipliers) decrease considerably.

The performance of the method has been demonstrated through nonlinear electrical and thermal problems. Accurate results are obtained with respect to some reference solutions obtained by meshing all the heterogeneities at lower computational costs.

References

[1] R. Blumenfeld, D.J. Bergman, Phys. Rev. B 40 (1989) 1987–1989.
[2] R. Blumenfeld, D.J. Bergman, Phys. Rev. B 44 (1991) 7378–7386.
[3] S. Pecullan, L.V. Gibiansky, S. Torquato, J. Mech. Phys. Solids 47 (1999) 1509–1542.
[4] P. Ponte Castañeda, M. Kailasam, Proc. R. Soc. Lond. A 453 (1997) 793–816.
[5] J. Chen, J. Cui, Appl. Numer. Math. 50 (2004) 1–13.
[6] M. Kamiński, Int. J. Eng. Sci. 41 (2003) 1–29.
[7] F. Feyel, J.L. Chaboche, Comput. Methods Appl. M. 183 (2000) 309–330.
[8] F. Feyel, Comput. Methods Appl. M. 192 (2003) 3233–3244.
[9] V.G. Kouznetsova, M.G.D. Geers, W.A.M. Brekelmans, Comput. Methods Appl. Mech. Eng. 193 (2004) 5525–5550.
[10] K. Matsui, K. Terada, K. Yuge, Comput. Struct. 82 (2004) 593–606.
[11] R.J.M. Smit, W.A.M. Brekelmans, H.E.H. Meijer, Comput. Methods Appl. M. 155 (1998) 181–192.
[12] J. Yvonnet, Q.-C. He, J. Comput. Phys. 223 (2007) 341–368.
[13] E.N. Lorenz, Empirical orthogonal eigenfunctions and statistical weather prediction, Technical Report, MIT, Department of Meteorology, 1956. (Statistical forecasting project).
[14] P. Krysl, S. Lall, J.E. Marsden, Int. J. Numer. Meth. Eng. 51 (4) (2001) 479–504.
[15] Y.C. Liang, H.P. Lee, S.P. Lim, W.Z. Lin, K.H. Lee, J. Sound Vib. 252 (3) (2002) 527–544.
[16] M.M. Loève, Van Nostrand, NJ, 1955.
[17] J.T. Oden, J.N. Reddy, Wiley-Interscience, New York, 1976.
[18] T.J.R. Hughes, Prentice-Hall, New Jersey, 1987.
[19] J.E. Marsden, T.J.R. Hughes, Dover, New York, 1994.
[20] M. Tanaka, T. Matsumoto, S. Takakuwa, Comput. Methods Appl. M. 195 (2006) 4953–4961.
[21] T. Arima, S. Yamasaki, K. Yamahira, K. Idemitsu, Y. Inagaki, C. Degueldre, J. Nucl. Mater. 352 (2006) 309–317.
[22] R. Barea, M. Belmonte, M.I. Osendi, P. Miranzo, J. Eur. Ceram. Soc. 23 (2003) 1773–1778.